Surface-Step-Induced Double Magnetic Switching of Fe on Vicinal W(100)

Hector C. Mireles* and J. L. Erskine

Department of Physics, The University of Texas at Austin, Austin, Texas 78712-1081

(Received 7 August 2000; published 27 June 2001)

Two-level magnetic switching of a bilayer epitaxial Fe film grown on a graded stepped W(100) surface is observed using the magneto-optic Kerr effect. Hysteresis loops produced by the film at a location on the curved W(100) surface corresponding to a vicinal angle of 6.4° exhibit two abrupt jumps in magnetization following spin orientation perpendicular to the steps resulting from surface-step-induced anisotropy. The two-step process can be understood in terms of abrupt depinning of spins in two inequivalent microdomains associated with the stepped surface. The results suggest a new realm of ultrathin film micromagnetics in which characteristic dimensions of 20–30 Å can play a dominant role.

DOI: 10.1103/PhysRevLett.87.037201 PACS numbers: 75.30.Gw, 78.20.Ls

Recent studies of ultrathin magnetic films on vicinal surfaces have revealed a rich variety of novel behavior that results from broken symmetry associated with surface atomic steps. Néel [1] proposed in 1954 a model of magnetic anisotropy based on reduced symmetry that predicted new magnetic anisotropy energies associated with a surface (loss of translational invariance perpendicular to the surface) and with the reduction of symmetry in the surface plane resulting from (for example) the introduction of periodic atomic steps by cutting the crystal at a vicinal angle. Perpendicular anisotropy [2,3] in ultrathin magnetic films, first observed by Gradmann and Müller [2] in 1968, and associated phenomena including reorientation transitions are manifestations of magnetic thin film surface anisotropy. Surface-step-induced anisotropy was first invoked in 1987 to account for features observed in spin-wave data [4] for Fe ultrathin films on W(110) and was later, in 1992, directly observed in experiments involving ultrathin ferromagnetic films grown on vicinal surfaces of Cu(111) [5] and W(100) [6].

Chung, Ballentine, and O'Handley [7] extended the Néel model and applied it to explain primary features of surface-step-induced anisotropy in the Fe/W(100) and Co/Cu(111) systems. Additional experimental studies [8,9] of other systems including Fe on Ag(100) and Pd(100) have verified Néel model predictions. More recently, Hyman, Zangwill, and Stiles (HZS) [10] have introduced and explored the "anisotropy phase diagram" of ultrathin magnetic films on vicinal surfaces based on a one-dimensional micromagnetic model that incorporates domain wall exchange energy (J) with bulk (K_4) and step (K_2) anisotropy energies. While conducting experiments to test HZS model predictions (that will be reported in a future publication) we discovered a novel switching phenomenon associated with ultrathin Fe films on vicinal W(100) surfaces that is reported in this Letter.

Figure 1 displays selected hysteresis loops for 2 monolayer (ML) thick $p(1 \times 1)$ Fe films, on two types of vicinal W(100) surfaces, measured using the magneto-optic Kerr effect (MOKE). Loops (a), (b), and (c) were measured on flat vicinal surfaces prepared by polishing a W(100) surface to produce three accurately aligned faces: a (100) face and two vicinal faces $(0, 1, 8)$ and $(0, 1, 10)$. Loops (d) and (e) and others not displayed were measured on a second W(100) crystal prepared to have a flat (100) face at one edge, and a graded-step-density region produced by a cylindrically shaped surface. In our experiments using the graded-step-density surface, the 1 mm diameter laser beam was focused to a small spot (~0.1 mm diameter) by a lens outside of the vacuum chamber. All loops were measured using the longitudinal MOKE configuration [11] in which the applied field lies in the plane of incidence. The sample was oriented with step edges parallel to the applied field; the surface-step-induced uniaxial anisotropy of Fe on vicinal W(100) produces a remanent in-plane magnetization perpendicular to the steps.

The light-polarization dependence of loops (a) and (b) and the vicinal-angle dependence of loops (a), (c), and (d) are manifestations of in-plane surface-step-induced magnetic anisotropy. Hysteresis loops (a), (c), and (d) obtained using s-polarized light and the longitudinal MOKE configuration [11] measure the in-plane magnetization component parallel to the plane of incidence averaged over the area of illumination. Hysteresis loop (b) measured using p-polarized light is a manifestation of the transverse MOKE in which the magnetic response is proportional to the magnetization perpendicular to the plane of incidence. Thus loops (a) and (b) illustrate how the polarization dependence of the MOKE can be used to probe the in-plane magnetic anisotropy. A third configuration (polar MOKE) in which the applied field perpendicular to the surface can produce perpendicular magnetization can be used to probe perpendicular anisotropy. No polar MOKE signals were detected in our current studies of 2 ML $p(1 \times 1)$ Fe on W(100) or in prior experiments [6], and polarized electron emission experiments [12] have confirmed that the shape anisotropy confines the magnetization in-plane and that the surface-step-induced anisotropy for 2 ML Fe films on W(100) produces in-plane remanent magnetization perpendicular to step edges.

Loop (e), corresponding to vicinal angle $\alpha = 6.4°$, exhibits four abrupt changes in magnetization at

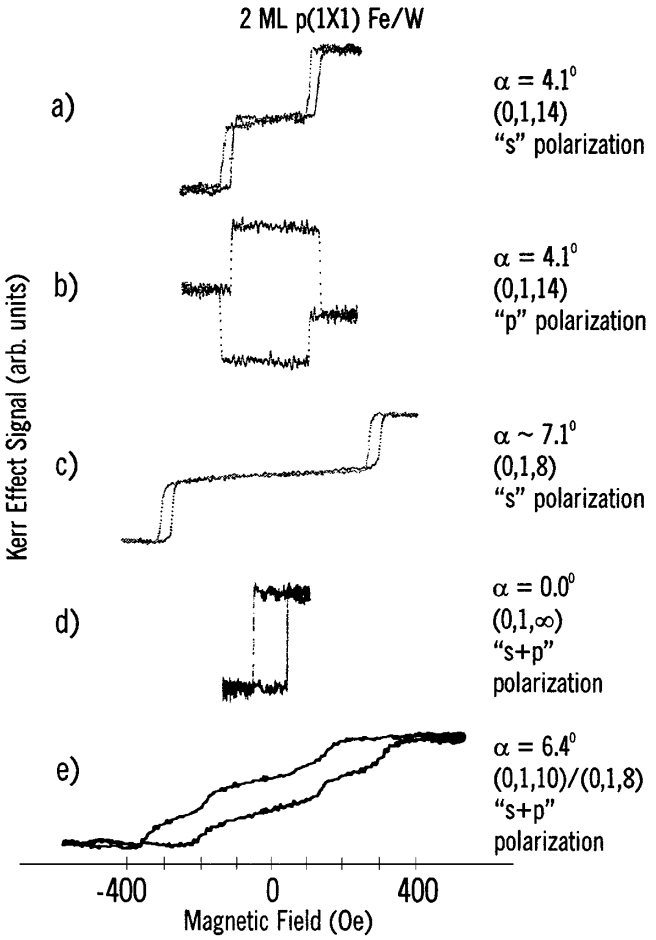

FIG. 1. Hysteresis loops for 2 ML $p(1 \times 1)$ Fe on W(100) measured using the MOKE. Films for (a), (b), and (c) were grown on flat vicinal surfaces. Films for (d) and (e) were grown on a graded stepped surface. The polarization difference between (a) and (b) is a manifestation of spin orientation perpendicular to steps driven by surface-step-magnetic anisotropy (refer to text). The vicinal angle α and plane index are indicated for each loop. Two-level switching at $H \sim \pm 175$ Oe and ± 350 Oe is apparent for $\alpha = 6.4°$ [loop (e)].

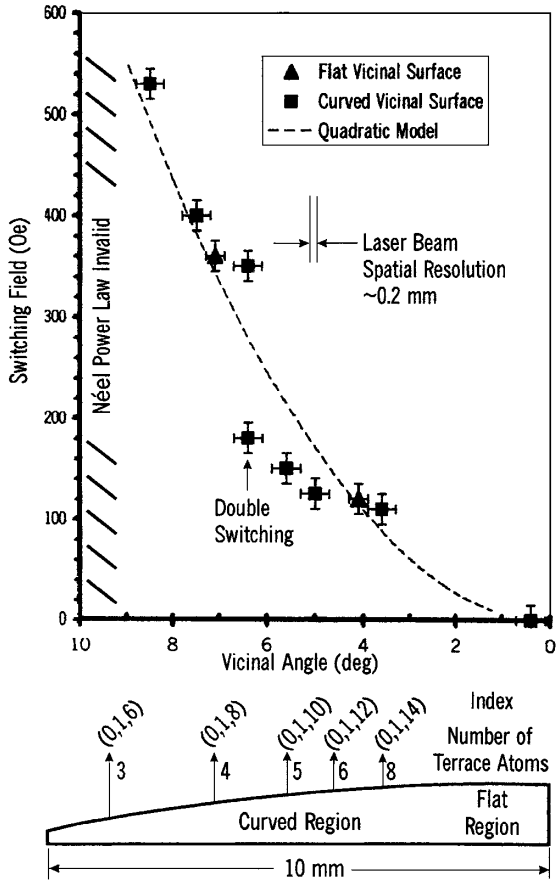

FIG. 2. Plot of switching field H_s vs vicinal angle α. Solid points, experimental data; dashed line α^2 dependence predicted by the Néel model. Shaded region for $\alpha > 9°$; switching field no longer obeys α^2 law. The crystal profile with the location of high-index regions referenced to the vicinal angle of the plot is shown below the graph.

$H = \pm 175$ Oe and $H = \pm 350$ Oe. This loop was measured with a small component of p polarization to reveal evidence of the transverse MOKE contribution [refer to (b)], around $H = 0$ produced by the step-induced anisotropy. We note that $\alpha = 6.4°$ lies halfway between angles $\alpha = 7.12°$ and $\alpha = 5.71°$ that correspond to plane indices $(0, 1, 8)$ and $(0, 1, 10)$. These surfaces have terrace widths containing $N = 4$ and $N = 5$ atoms, respectively. Loop (e) suggests the existence of an intermediate state of magnetization between $H = \pm 175$ and ± 350 Oe in which the component of M parallel to H averaged over the beam area is about one-half of M_s, the saturated magnetization.

Figure 2 compares our experimental results with the quadratic dependence of H_s vs α predicted by the Néel model [8] by plotting H_s vs α. Data points obtained from flat vicinal surfaces are in good agreement with corresponding data obtained from the graded-vicinal surface suggesting that the use of a graded surface to measure $H_s(\alpha)$ is valid. The size of the laser beam spot in relation to the gradient of steps on the curved W(100) surface can be judged from Fig. 2 which indicates that if the crystal step distribution is regular, the beam averages over a very narrow range of step widths.

The magnetic characteristics of our 2 ML $p(1 \times 1)$ Fe films on vicinal W(100) (Figs. 1 and 2) are in good agreement with prior MOKE [6,9] and polarized electron [12] experiments that have been attributed to in-plane surface-step-induced magnetic anisotropy. We attribute the double switching observed at $\alpha = 6.4°$ to a surface region having approximately an equal number of $N = 4$ and $N = 5$ atom terraces. With this assumption, all of the measured switching fields fall reasonably close to a curve described by $H_c \sim \alpha^2$. Other features of our results are generally compatible with HZS and Néel model predictions: the variation (decrease) of $H_s(\alpha)$ as a function of film thickness or surface contamination by oxygen and the effect of these parameters plus terrace width on loop shapes (loop phase diagram features).

The double magnetic switching, observed at $\alpha = 6.4°$, can be understood based on the vicinal angle dependence of H_s established in Fig. 2 and the tendency of a W(100) vicinal crystal cut at an angle between two high-index planes to adopt a structure characteristic of the average of the two planes (Fig. 3). If we assume that the $p(1 \times 1)$ Fe structures on each terrace behave as individual microdomains and switch at the fields $H_s(\alpha)$ given by Fig. 2, both of the primary features of the double switching loop are accounted for: the measured values of the two switching fields and the relative magnitude of each transition (about $1/2M_s$).

Our measurements indicate that the Néel quadratic power law behavior becomes invalid abruptly beyond $\alpha \sim 8.5°$ (H_s stops increasing) and beyond $\alpha = 12°$, the loops collapse to a shape similar to those measured at $\alpha = 0$ [Fig. 1, loop (d)]. Thus double switching will not be observed at $\alpha = 8.3°$ corresponding to a stepped surface having $N = 3$ and $N = 4$ terraces. At smaller vicinal angles (larger terrace sizes) it becomes increasingly more difficult to observe the double switching because of the α^2 dependence of H_s. These factors may account for the fact that we have observed clear evidence of double switching behavior only at $\alpha \sim 6.4°$. The quality of the stepped surface determines the sharpness of the switching behavior. This is apparent from the loops displayed in Fig. 1. The fixed-angle vicinal surfaces typically yield sharper LEED patterns (narrower distribution of terrace widths) than the graded-step-density surface, and the magnetic transitions are observed to be sharper.

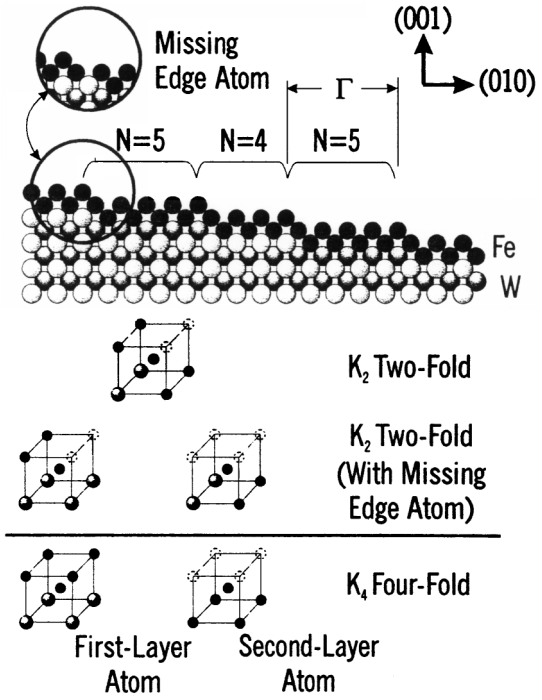

FIG. 3. Idealized surface structure model for 2 ML $p(1 \times 1)$ Fe on W(100). Circled regions show two local geometries at the step edge, one involving a missing atom. Both models provide atomic coordination that yields twofold anisotropy. The missing atom model should produce weaker interterrace coupling.

We now address the critical surface structure issue: How well is the model surface (Fig. 3) realized in our experiments? We have used high resolution spot-profile-analysis low-energy electron diffraction (SPALEED) to characterize the W(100) substrates, and commercial (Omicron) LEED and (VSW) Auger instruments available in our MOKE/film growth chamber for structure and chemical analysis of the films. The spot splitting from steps at $\alpha \sim 6.5°$ is easily resolved with a commercial LEED instrument and a more quantitative analysis was possible with our SPALEED system [13]. The spatial region probed by the MOKE polarimeter and the LEED systems is comparable (about 0.1 mm diameter). Also, the characteristic magnetic scale in the thin film systems is the exchange length $w = \sqrt{J/2K_4}$ which is estimated to be in the range of 10–50 Å. The coherence lengths of the commercial LEED (~100 Å) and SPALEED (>650 Å) systems are well suited for characterizing the surface structure on these spatial scales.

Figure 4 displays a representative LEED spot profile obtained from the graded-step-density surface showing the splitting that results from the terraces. These results show that the quality of the surface on the scale most important to the magnetic experiments is good: The well-resolved splitting in the region of vicinal angles where the double magnetic switching is observed is a manifestation of a narrow distribution of step widths (refer to Fig. 4).

Scanning tunneling microscopy (STM) analysis of conventionally prepared vicinal tungsten surfaces [14,15] reveals a small degree of lateral step width fluctuations along the terraces consistent with the LEED results displayed in Fig. 4. The STM studies also show that the terraces can extend hundreds of nanometers parallel to the steps. Corresponding STM images for vicinal Cu(111) surfaces [16] suggest that softer metal surfaces produce a broader distribution of terrace widths. On a length scale appropriate to the present discussion (250 Å) the idealized structure model (Fig. 4) should be valid for $p(1 \times 1)$ Fe on vicinal W(100).

There is extensive literature covering the structure and stability of single crystal metal surfaces including instabilities and surface structural phase changes (roughening transitions and phase separation into flat and bunched-step regions) that are particularly important on vicinal surfaces [17]. Our LEED studies of vicinal W(100) for $\alpha < 10°$ do not reveal any evidence of structural changes or instabilities resulting from our sample cleaning procedures that would invalidate the structure model adopted (Fig. 3) to interpret the vicinal angle switching dependence of Fig. 2. The uniform α^2 dependence of H_s extending to $\alpha \sim 9°$ and the agreement of this dependence with predictions of the Néel model is additional indirect but strong evidence of the validity of both the model that explains the double

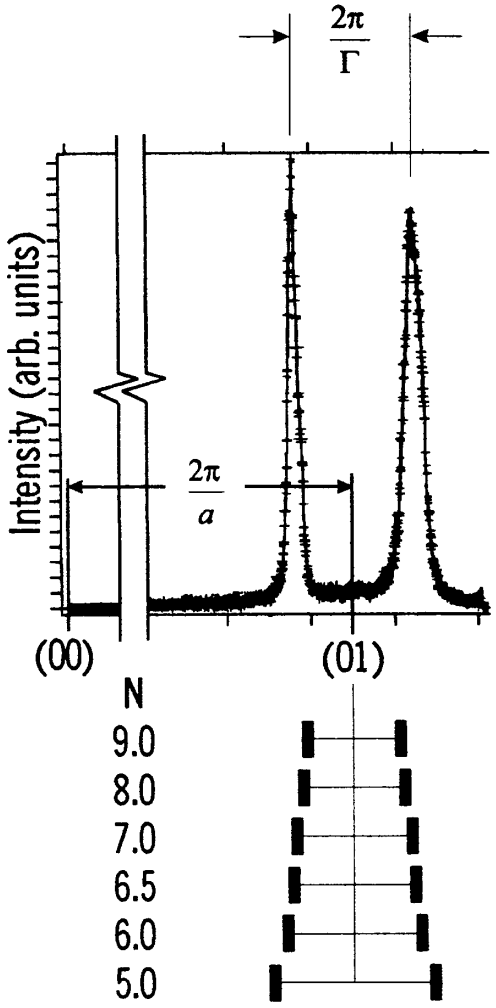

FIG. 4. Upper panel, spot profile LEED showing splitting of a 01 beam at $\alpha \sim 4.2°$ corresponding to a terrace width $\Gamma \sim 21$ Å and $N = 6.8$ atoms per terrace. Histograms below the graph illustrate instrument resolution (width of histogram bars correspond to FWHM of instrument response) and locations of split peaks for terraces ranging from $N = 5$ to $N = 9$.

magnetic switching and the structural basis for the model being achieved in the experiments.

In summary, we have observed double magnetic switching of Fe on vicinal W(100) and have connected the new phenomenon with the well-established phenomena of surface-step-induced anisotropy. The observed switching fields associated with the proposed double switching mechanism are generally compatible with the Néel mechanism that accounts for the uniaxial anisotropy. The micromagnetic domains associated with the terrace regions of the stepped surface appear to be compatible with micromagnetic simulations [10] that describe magnetic hysteresis in uniform films on stepped surfaces and with domain wall processes in sequesilayer systems [18]. Alternative switching models could apply to the experimental observation of two-state magnetic switching. Novel switching behavior that is essentially identical to the two-state switching reported here [Fig. 1(e)] was recently predicted [19] based on magnetostatically coupled single-domain particles. While the magnetic and structural characterization that we report (and relevant length scale) is compatible with the step-induced anisotropy mechanism we use to explain the double switching, we have no experimental evidence that would rule out switching by coupled single-domain regions on a different spatial scale (greater than a step width but smaller than 100 μm).

This work was supported by NSF DMR-9972113 and the Robert A. Welch Foundation.

*Current address: Physics Department, Trinity University, San Antonio, TX 78212.

[1] L. Néel, J. Phys. Radium **15**, 225 (1954).
[2] V. Gradmann and J. Müller, Phys. Status Solidi **27**, 313 (1968).
[3] B. T. Jonker, K.-H. Walker, E. Kisker, G. A. Prinz, and C. Carbone, Phys. Rev. Lett. **57**, 142 (1986); J. G. Gay and R. Richter, Phys. Rev. Lett. **56**, 2728 (1986).
[4] B. Hillebrands, P. Baumgart, and G. Guntherodt, Phys. Rev. B **36**, 2450 (1987).
[5] A. Berger, U. Linke, and H. P. Oepen, Phys. Rev. Lett. **68**, 839 (1992).
[6] J. Chen and J. L. Erskine, Phys. Rev. Lett. **68**, 1212 (1992).
[7] D. S. Chung, C. A. Ballentine, and R. C. O'Handley, Phys. Rev. B **49**, 15 084 (1994).
[8] R. K. Kawakami, E. J. Escorcia-Aparicio, and Z. Q. Qiu, Phys. Rev. Lett. **77**, 2570 (1996).
[9] H. J. Choi, R. K. Kawakami, E. J. Escorcia-Aparicio, Z. Q. Qiu, J. Pearson, J. S. Jiang, D. Li, R. M. Osgood III, and S. D. Bader, J. Appl. Phys. **85**, 4958 (1999).
[10] R. A. Hyman, A. Zangwill, and M. D. Stiles, Phys. Rev. B **58**, 9276 (1998).
[11] A. V. Sokolov, *Optical Properties of Metals* (American Elsevier Publishing Co., New York, 1967).
[12] D.-J. Huang, J. Lee, G. A. Mulhollan, and J. L. Erskine, J. Appl. Phys. **73**, 1 (1993).
[13] F. K. Men, B. L. Clothier, and J. L. Erskine, Rev. Sci. Instrum. **64**, 1883 (1993).
[14] M. Getzlaff, R. Pascal, H. Todter, M. Bode, and R. Wiesendanger, Surf. Rev. Lett. **6**, 241 (1999).
[15] H. Bethge, D. Hener, Ch. Jensen, K. Reshöft, and V. Köhler, Surf. Sci. **331**, 878 (1995).
[16] J. Shen, M. Klana, P. Ohresser, H. Jenniches, J. Parthel, Ch. V. Mohan, and J. Kirschner, Phys. Rev. B **56**, 11 134 (1997).
[17] For example, refer to the review by E. H. Conrad, Prog. Surf. Sci. **39**, 66 (1992).
[18] M. Kolesik, M. A. Novotny, and P. A. Rikvold, Phys. Rev. B **56**, 11 791 (1997).
[19] R. L. Stamps and R. E. Camley, Phys. Rev. B **60**, 11 694 (1999).